Article

Crystal Structures of Wild-type and F448A Mutant Citrobacter freundii Tyrosine Phenol-lyase Complexed with Substrate and Inhibitors: Implications for the Reaction Mechanism

Robert S Phillips, and Steven Craig

Biochemistry, **Just Accepted Manuscript** • DOI: 10.1021/acs.biochem.8b00724 • Publication Date (Web): 27 Sep 2018

Crystal Structures of Wild-type and F448A Mutant *Citrobacter freundii* Tyrosine Phenol-lyase Complexed with Substrate and Inhibitors: Implications for the Reaction Mechanism

Robert S. Phillips*[‡§] and Steven Craig[§]

Departments of Chemistry[‡] and Biochemistry and Molecular Biology[§], University of Georgia, Athens, GA 30602

*To whom correspondence should be addressed at Department of Chemistry, University of Georgia, Athens, GA 30602. Phone: (706) 542-1996 Fax: (706) 542-9454 Email: plp@uga.edu

Abstract

Tyrosine phenol-lyase (TPL; E.C. 4.1.99.2) is a pyridoxal-5'-phosphate dependent enzyme that catalyzes the reversible hydrolytic cleavage of L-tyrosine to phenol and ammonium pyruvate. We have shown previously that F448A TPL has k_{cat} and k_{cat}/K_m values for L-tyrosine reduced by about 10^4 (Phillips, R. S., Vita, A., Spivey, J. B., Rudloff, A. P., Driscoll, M. D., & Hay, S. (2016) *ACS Catalysis*, *6*, 6770-6779). We have now obtained crystal structures of F448A TPL and complexes with L-alanine, L-methionine, L-phenylalanine, and 3-F-L-tyrosine at 2.05-2.27 Å, as well as the complex of wild-type TPL with L-phenylalanine at 1.8 Å. The small domain of F448A TPL, where Phe-448 is located, is more disordered in chain A than wild-type TPL. The complexes of F448A TPL with L-alanine and L-phenylalanine are in an open conformation in both chains, while the complex with L-methionine is a 52:48 equilibrium mixture of open and closed conformations, respectively, in chain A. Wild-type TPL with L-alanine is closed in chain A and open in chain B, and the complex with L-phenylalanine is 56:44 in open and closed conformations in chain A. Thus, the Phe-448 to alanine mutation affects the conformational equilibrium of open and closed active sites. The structure of the 3-F-L-tyrosine quinonoid complex of F448A TPL is unstrained and in an open conformation, with a hydrogen bond from the phenolic OH to Thr-124. These results support our previous conclusion that ground-state strain plays a critical role in the mechanism of TPL.

Introduction

Tyrosine phenol-lyase (TPL[1], EC 4.1.99.2) is a pyridoxal-5'-phosphate (PLP) dependent enzyme that catalyzes the reversible β-elimination of L-tyrosine to give phenol and ammonium pyruvate (Eqn. 1) (1). In addition to L-tyrosine, other amino acids with good leaving groups on the β-carbon, such as S-(*o*-nitrophenyl)-L-cysteine (SOPC), are substrates for irreversible eliminations (Eqn. 2). The elimination of a formally unactivated carbon leaving group in the reaction of TPL is

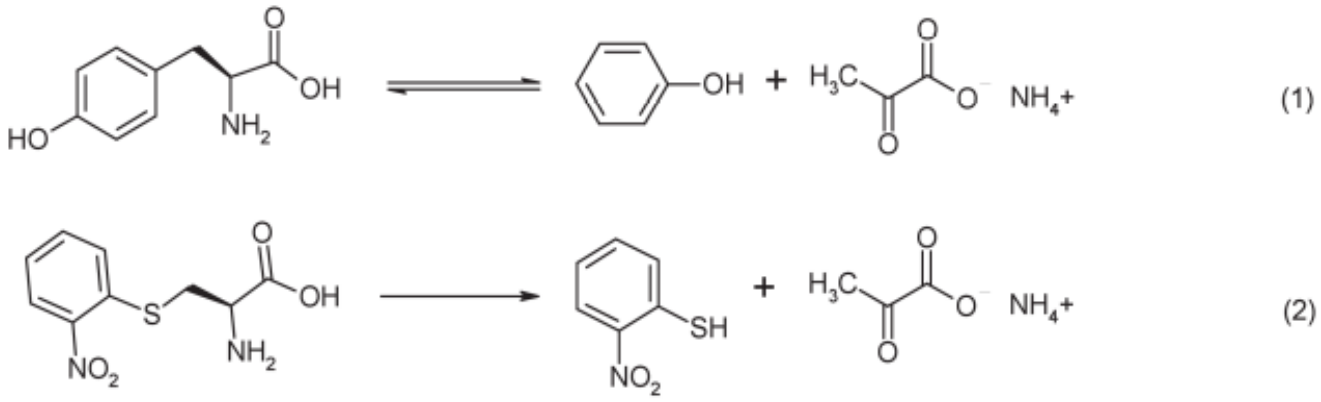

mechanistically interesting. Mechanisms have been proposed utilizing general acid-base catalysis via a high energy tautomeric cyclohexadienone intermediate (2-6). The crystal structures of Y71F and F448H TPL complexed with 3-F-L-tyrosine show that the bound substrate is in a strained geometry, with the phenyl ring bent ~20° out of plane with the C_β-C_γ bond (7). In this strained complex, the phenolic OH of the substrate forms hydrogen bonds to Arg-381 and Thr-124, while Phe-448 and Phe-449 move into the active site in close contact to the phenyl ring of the substrate. This suggested that ground-state strain contributes significantly to TPL catalysis. Mutagenesis of Phe-448 to alanine and leucine and of Phe-449 to alanine resulted in ~10^4 loss of activity with L-tyrosine, but not with SOPC and S-ethyl-L-cysteine (8), consistent with the proposed role of these residues in introducing steric strain into L-tyrosine. We have now obtained x-ray crystal structures of F448A TPL and complexes with L-alanine, L-methionine, L-phenylalanine, and 3-F-L-tyrosine, as well as the structure of wild-

1 Abbreviations are: TPL, tyrosine phenol-lyase; PLP, pyridoxal-5'-phosphate; SOPC, S-(o-nitrophenyl)-L-cysteine

type TPL complexed with L-phenylalanine. These structures support our previous conclusion that Phe-448 contributes to TPL catalysis by causing ground state strain in the bound substrate.

Materials and methods

Enzymes and crystals. Wild-type and F448A TPL were expressed and purified as previously described (8, 9). Crystals were prepared as described previously, using hanging drops with wells containing 0.05 M triethanolamine-HCl, pH 8.0, 0.2 M KCl, 1 mM dithiothreitol, 0.1 mM PLP, and 36-40% PEG 5000 MME (7, 10). The protein solution, 2 µL of 15 mg/mL in the same buffer, was mixed with 2 µL of the precipitant solution on a polystyrene cover slip and sealed with petroleum jelly over 1 mL of the precipitant solution in the well. Crystals grew at room temperature (20-22 ºC) in 2-4 weeks as yellow prisms.

Data collection and analysis. The crystals were soaked in a cryoprotection solution containing 0.05 M triethanolamine-HCl, pH 8.0, 0.2 M KCl, 1 mM dithiothreitol, 0.1 mM PLP, 40% PEG 5000 MME, and 20% (v/v) of cryoprotectant, ethylene glycol:dimethyl sulfoxide:glycerol (1:1:1), and flash-cooled in liquid nitrogen. For ligand soaks, the crystals were incubated in the cryoprotectant solution containing 0.1 M L-alanine, 0.04 M L-methionine, 0.1 M L-phenylalanine, or 0.02 M 3-F-L-tyrosine for 1-2 minutes before flash-cooling. Diffraction data were collected at the SER-CAT ID-22 or BM-22 beamlines at Argonne National Laboratory. Data were collected at 100 K for 360º with 0.5º or 1.0º oscillations. The data were integrated with XDS (11) and scaled and merged with XSCALE (11). Resolution limits were determined by CC(1/2) ~ 0.3, and the paired refinement technique (12). Phasing was performed by molecular replacement with PHASER (13) using 2TPL.pdb, 2VLF.pdb or 2VLH.pdb as the search models. Model building was performed, and water and ligands were added, with COOT (14). The disorder in chain A was modeled using the structure of the small domain from 2TPL.pdb for the open conformation and 2VLF.pdb for the closed conformation. The open conformation was assigned to ALT.LOC A, while the closed was assigned to ALT.LOC B, in the pdb file. Initial occupancies for both conformations before refinement were set to 0.5. Ligands were built

with CHEM3D (Cambridge Biosoft) and converted to cif format with PHENIX.ELBOW. The ligands were assigned as quinonoid or aldimine structures based on which structure gave the least difference density in the mFo-DFc maps. The models were refined with PHENIX.REFINE (15) using TLS and NCS. TLS assignments were done with PHENIX.find_tls_groups. The statistics for the final structures are summarized in Table 1. The figures were prepared with PYMOL 1.8.4 (Schrodinger, LLC).

Table 1. Data collection and refinement statistics.

Entry	6DXV (F448A TPL)	6DYT (F448A TPL-L-alanine)	6ECG (F448A TPL-L-methionine	6DUR (Wild-type TPL-L-phenylalanine)	6DVX (F448A TPL-L-phenylalanine)	6DZ5 (F448A TPL-3-F-L-tyrosine)
Wavelength	1.0000 Å	1.0000 Å	1.0000 Å	1.0000 Å	1.0000 Å	1.0000 Å
Resolution range (Å)	36.25 - 2.2 (2.279 - 2.2)	37.88 - 2.05 (2.123 - 2.05)	45.95 - 2.27 (2.351 - 2.27)	48.73 - 1.8 (1.864 - 1.8)	37.75 - 2.27 (2.351 - 2.27)	44.47 - 2.26 (2.341 - 2.26)
Space group	P 2 21 21	P 2 21 21	P 2 21 21	P 2 21 21	P 2 21 21	P 2 21 21
Unit cell (Å, Å, Å, °, °, °)	59.35 132.18 145.01 90 90 90	59.64 133.27 145.07 90 90 90	59.61 132.85 144.27 90 90 90	59.51 133.33 142.84 90 90 90	59.78 132.67 144.97 90 90 90	59.88 132.81 145.37 90 90 90
Total reflections	345973 (34799)	367402 (38240)	323030 (32841)	1408165 (76677)	800773 (80249)	795217 (81190)
Unique reflections	58142 (5733)	72651 (7218)	53790 (5280)	105085 (9671)	54164 (5342)	54533 (5432)
Multiplicity	6.0 (6.0)	5.1 (5.3)	6.0 (6.2)	13.4 (7.9)	14.8 (15.0)	14.6 (14.9)
Completeness (%)	96.23 (75.46)	99.27 (99.00)	99.92 (99.91)	98.64 (89.45)	99.73 (99.72)	98.68 (99.89)
Mean I/sigma(I)	7.14 (0.41)	6.91 (0.47)	7.75 (0.59)	12.47 (0.53)	13.21 (0.88)	11.18 (0.87)
Wilson B-factor ($Å^2$)	47.59	56.87	42.36	33.65	54.62	51.32
R-merge	0.1218 (4.86)	0.1046 (3.39)	0.1189 (3.433)	0.1246 (3.427)	0.1677 (3.886)	0.2269 (3.346)
R-meas	0.1338 (5.334)	0.1171 (3.773)	0.1307 (3.751)	0.1295 (3.666)	0.1737 (4.022)	0.2352 (3.464)
R-pim	0.05459 (2.174)	0.05105 (1.613)	0.05322 (1.495)	0.03467 (1.262)	0.04505 (1.03)	0.06152 (0.8925)
CC1/2	0.997 (0.469)	0.997 (0.155)	0.997 (0.239)	0.999 (0.302)	0.999 (0.403)	0.998 (0.341)
CC*	0.999 (0.799)	0.999 (0.517)	0.999 (0.621)	1 (0.681)	1 (0.758)	1 (0.713)

Reflections used in refinement	56562 (4366)	72869 (7155)	53792 (5278)	104562 (9362)	54040 (5331)	54458 (5428)
Reflections used for R-free	1950 (151)	1997 (187)	2005 (196)	1992 (180)	1997 (198)	1998 (197)
R-work	0.2161 (0.7018)	0.1864 (0.3758)	0.1831 (0.2985)	0.1720 (0.3515)	0.1820 (0.3929)	0.1837 (0.3381)
R-free	0.2562 (0.7001)	0.2322 (0.3974)	0.2204 (0.3428)	0.1933 (0.3759)	0.2167 (0.4210)	0.2206 (0.3724)
CC(work)	0.962 (0.177)	0.951 (0.401)	0.880 (0.463)	0.967 (0.602)	0.972 (0.682)	0.965 (0.613)
CC(free)	0.922 (0.281)	0.947 (0.336)	0.852 (0.454)	0.962 (0.615)	0.955 (0.691)	0.954 (0.381)
Number of non-hydrogen atoms	7696	7940	7911	8060	7800	7886
macromolecules	7182	7251	7163	7331	7203	7242
ligands	2	66	58	88	78	82
solvent	512	623	690	641	519	562
Protein residues	903	912	900	907	905	909
RMS(bonds) (Å)	0.007	0.004	0.0022	0.016	0.004	0.004
RMS(angles) (°)	0.98	0.95	0.454	1.49	0.94	0.93
Ramachandran favored (%)	98.09	98.01	97.55	97.78	96.99	97.56
Ramachandran allowed (%)	1.80	1.88	2.45	2.00	2.68	2.44
Ramachandran outliers (%)	0.11	0.11	0.00	0.22	0.33	0.00
Rotamer outliers (%)	1.88	0.79	1.55	1.55	1.20	0.79
Clashscore	4.21	2.83	4.9	4.82	4.30	2.96
Average B-factor (Å^2)	90.64	80.08	59.87	46.83	78.95	70.26
macromolecules	90.86	79.83	59.73	46.12	78.87	69.84
ligands	72.45	87.89	71.75	60.64	82.60	80.58
solvent	91.22	82.41	62.33	54.53	79.56	74.18
Number of TLS groups	8	15	11	10	11	10

Statistics for the highest-resolution shell are shown in parentheses.

Stopped-flow kinetics. Stopped-flow data were collected on an OLIS RSM-1000 rapid-scanning stopped-flow spectrophotometer for scanning and an Applied Photophysics SX-20 stopped-flow spectrophotometer for single wavelength measurements. The enzyme was applied to a PD-10 gel column (GE Healthcare) equilibrated with 0.05 M triethanolamine-HCl, pH 8.0, 0.2 M KCl to exchange buffer before use. The final concentration of enzyme was ~1 mg/mL for scanning and 0.5 mg/mL for single wavelength data collection. The single wavelength data were collected at 500 nm for L-alanine, 502 nm for L-phenylalanine, and 510 nm for 3-F-L-tyrosine, with a 2.3 nm bandpass. The data were collected at room temperature, 21 ± 1 ºC. The time course data were fit to two or three exponentials (Equation 3). The dependence of the apparent rate constants on the ligand concentrations were fit using Eqn. 4.

$$A_t = \Sigma A_i \exp(-k_i * t) + A_o \quad (3)$$

$$k_{obs} = k_f * [L]/(K_{eq}+[L]) + k_r \quad (4)$$

Results

Structure of F448A TPL. Crystals of F448A TPL were obtained under the same conditions as wild-type TPL (7), and the structure of F448A mutant TPL was determined to a resolution of 2.2 Å. The asymmetric unit of TPL is a homodimer, although the biological assembly is a homotetramer. The Cα backbone is nearly superposable with that of wild-type TPL (Figure 1A), with an RMSD of 0.549. However, the small domain (residues 19–44, 346–404, and 434–456) of the A chain is more disordered compared to that of wild-type TPL (compare Figure S1A and S1B, top). The mobile loop of F448A

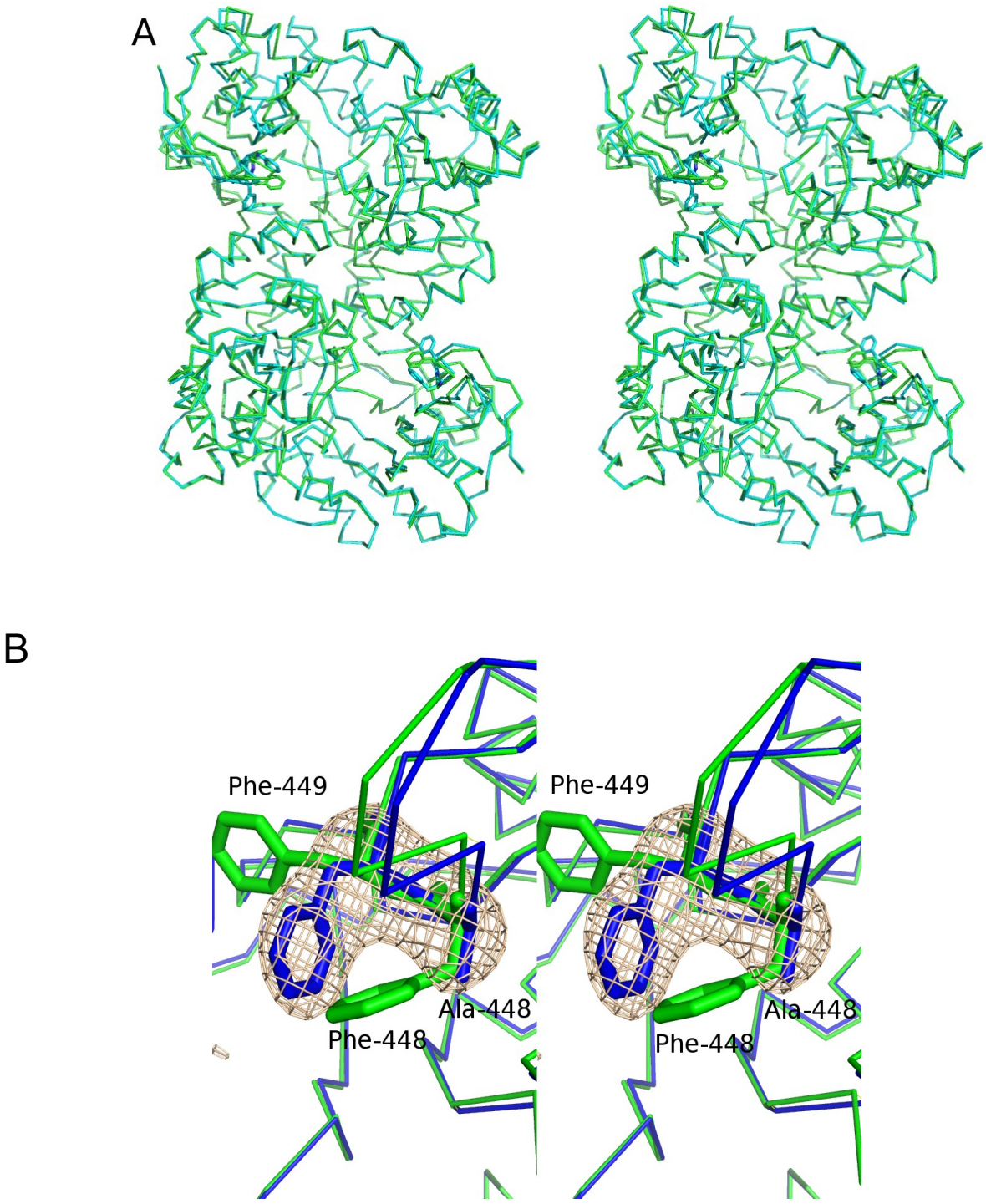

Figure 1. A. Crossed-eye stereo view of the overlay of structures of wild-type TPL (cyan) and F448A TPL (green). B. Crossed-eye stereo view of the conformation of F448 and F449 in chain A of wild-type TPL (green) and Ala-448 and Phe-449 in chain A of F448A TPL (blue), showing the simulated annealing omit mFo-DFc map for Ala-448 and Phe-449 at 4 σ.

TPL chain A containing residues 388-394 does not show sufficient density to fit. The side chain of Phe-449 is also in a different conformation in F448A TPL than wild-type TPL, rotated in toward the active site, possibly due to the reduced steric demands of the smaller alanine side chain of Ala-448 (Figure 1B). In contrast, chain B of F448A TPL is not significantly more disordered than wild-type TPL (compare Figure S1A and S1B, bottom). As expected, the electron density of the phenyl ring of Phe-448 is absent from the F448A TPL structure (Figure 1B). Thus, as we concluded previously from the kinetic properties of F448A TPL (8), the Phe-448 to alanine mutation has only minor effects on the overall structure of TPL.

Structure of F448A TPL complex with L-alanine. L-Alanine is a competitive inhibitor that reacts with TPL to form a quinonoid complex, and also undergoes a slow racemization reaction (7, 9, 16, 17). When crystals of F448A TPL were soaked in cryo solutions containing 100 mM L-alanine, the crystals changed from yellow to orange in color. The structure of the L-alanine complex of F448A TPL shows the expected quinonoid structure in chain A with trigonal geometry at C_α of the bound alanine (Figure 2A), but the electron density in chain B fits best to an external aldimine, with the C_α out of plane with the pyridine ring of PLP, and with a tetrahedral geometry relating the C_α, C_β and carboxylate (Figure 2B). This is in contrast to the stucture of wild-type TPL complex with L-alanine, which shows a quinonoid complex in both subunits of the asymmetric unit (7). Furthermore, chain A of the wild-type TPL complex with L-alanine is in a closed conformation, while chain B is in an open conformation. In the closed conformation of the wild-type TPL complex with L-alanine in chain A, the small domain has rotated toward the large domain, and the phenyl rings of both Phe-448 and Phe-449 move toward the bound ligand by 4.3 and 10.8 Å, respectively (7). In contrast, both subunits of F448A TPL complexed with L-alanine are in open conformations (Figure 2A, 2B). The side chain of Phe-449 adopts two conformations in chain B of the wild-type TPL complex, with the phenyl ring either flipped out or flipped in to the active site (Figure 2B, cyan), but chain B in F448A TPL shows only one conformation for Phe-449 (Figure 2B, green), flipped in.

Kinetics of L-alanine reaction with F448A TPL. Mixing F448A TPL with L-alanine results in formation of a new absorption peak at 500 nm, attributed to the quinonoid complex (Figure 3A), as well as a peak at about 400 nm for an aldimine complex. This is consistent with the structure in Figure 2 showing both quinonoid and aldimine complexes. The rate of formation of the quinonoid complex is concentration dependent (Figure 3B), and the progress curves were found to require three exponentials for an adequate fit to Eqn. 3. The rate constants and amplitudes from exponential fitting are shown in Figure 3C and 3D. The fast phase has the lowest amplitude, the second phase has a higher amplitude, and the slowest phase has the highest amplitude. The <2-fold variation in rates with [L-alanine] for the fast phase precludes a good fit of the data in Figure 3B to Eqn. 4, but k_{obs} for quinonoid intermediate

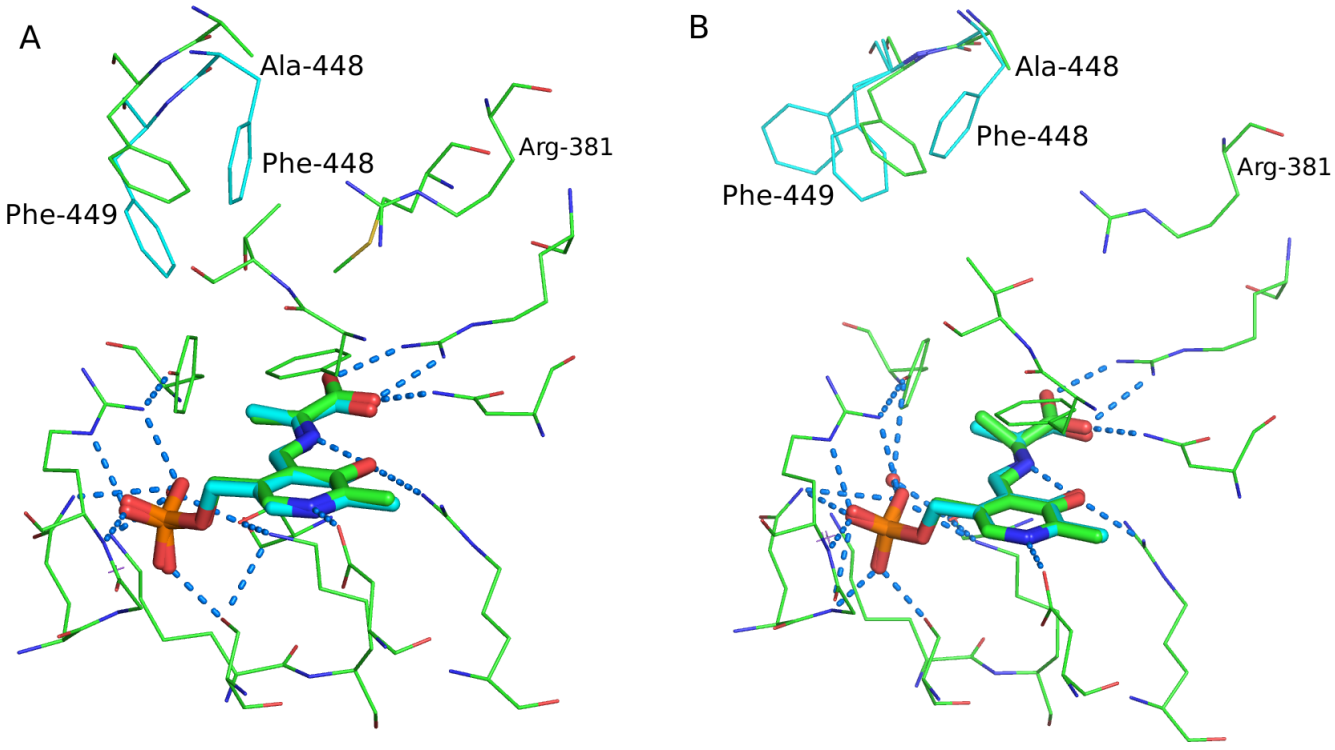

Figure 2. Structures of L-alanine bound to F448A TPL. F448A TPL is shown in green, and the Phe-448, Phe-449, and the alanine complex of the wild-type TPL structure wild-type TPL structure are shown in cyan. Potential hydrogen-bonds are indicated in blue dashes. A. Interactions of the PLP-L-alanine complex in chain A. B. Interactions of the PLP-L-alanine complex in chain B.

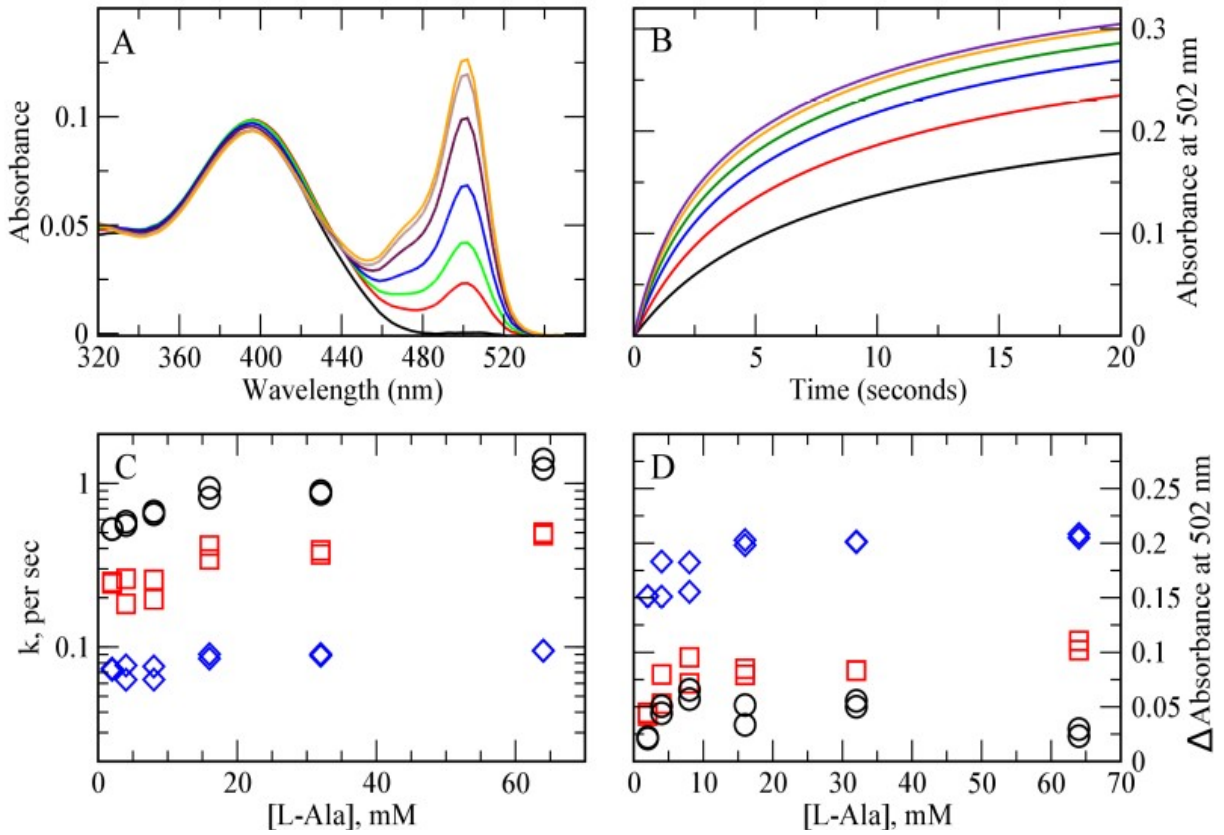

Figure 3. Stopped-flow kinetics of F448A TPL reaction with L-alanine. A. Rapid-scanning stopped-flow spectra of F448A TPL reaction with 0.1 M L-alanine. The scans are shown at 0.002 sec (black), 0.5 sec (red), 1 sec (green), 2 sec (blue), 4 sec (maroon), 8 sec (brown) and 12 sec (orange). B. Single-wavelength traces at 502 nm for the reaction at 2 (black), 4 (red), 8 (blue), 16 (green), 32 (orange), and 64 (brown) mM L-alanine. C. Rate constants for the reaction of L-alanine with F448A TPL fit to Eqn. 4 with three exponentials. Fast phase (○); intermediate phase (□); slow phase (◊). D. Amplitudes for the reaction of L-alanine with F448A TPL fit to Eqn. 4 with three exponentials. Fast phase (○); intermediate phase (□); slow phase (◊).

formation is about 1 s^{-1}. The kinetics of L-alanine reaction with F448A TPL are similar to previous results with wild-type TPL (17). The slowest phase shows little variation with [L-alanine] and has a rate constant of about 0.1 s^{-1}.

Structure of F448A TPL complex with L-methionine. The structure of the complex of wild-type TPL with L-methionine has been determined previously (7). In contrast to the structure of wild-type TPL complexed with L-alanine, L-methionine was found only in the active site of the A chain. In F448A TPL, we also found that the ligand is present only in the A chain. The electron density is consistent with a quinonoid structure (Figure S3A), as was found with wild-type TPL. The small domain of the A chain is disordered, and refinement required modeling of two conformations, open and closed, for residues 13-40, 347-377, and 421-456 (Figure S3B). These two conformations have occupancies of 48% and 52% for the closed and open states, respectively, in the refined structure. Phe-449 is found in two conformations, both of which are flipped in to the active site, but in neither conformation does it enter the active site as far as it does in the wild-type TPL complex with L-methionine (Figure 4, compare green and cyan structures). Thus, the mutation of Phe-448 to alanine affects the ability of the enzyme to form a closed active site conformation. The conformation of the side chain of the L-methionine ligand is also different for F448A TPL, with the methyl in an *anti*-orientation, compared to *syn* for wild-type TPL (Figure 4). This may be due to less steric restriction in the active site as a result of the F448A mutation.

Kinetics of L-methionine reaction with F44A TPL. Mixing of L-methionine with wild-type TPL results in a quinonoid complex with an absorption maximum at 506 nm (9). F448A TPL reacts with L-methionine to give a similar spectrum (Figure 5A). The rate constant of the reaction shows a concentration dependence on [L-methionine] (Figure 5B, 5C). In contast to the reaction of L-alanine, the progress curves of these reactions can be fit with only two exponential phases (Figure 5C). The fast phase fits well to Eqn. 4, with $k_f = 12.1 \pm 1.4$ s^{-1}, $k_r = 0.35 \pm 0.03$, and $K_d = 78.2 \pm 12.9$ mM. The slow

phase is independent of [L-methionine] and has k_{obs}~0.1 s^{-1}. The slow phase has a higher amplitude than the fast phase at concentrations of L-methionine below 30 mM (Figure 5D).

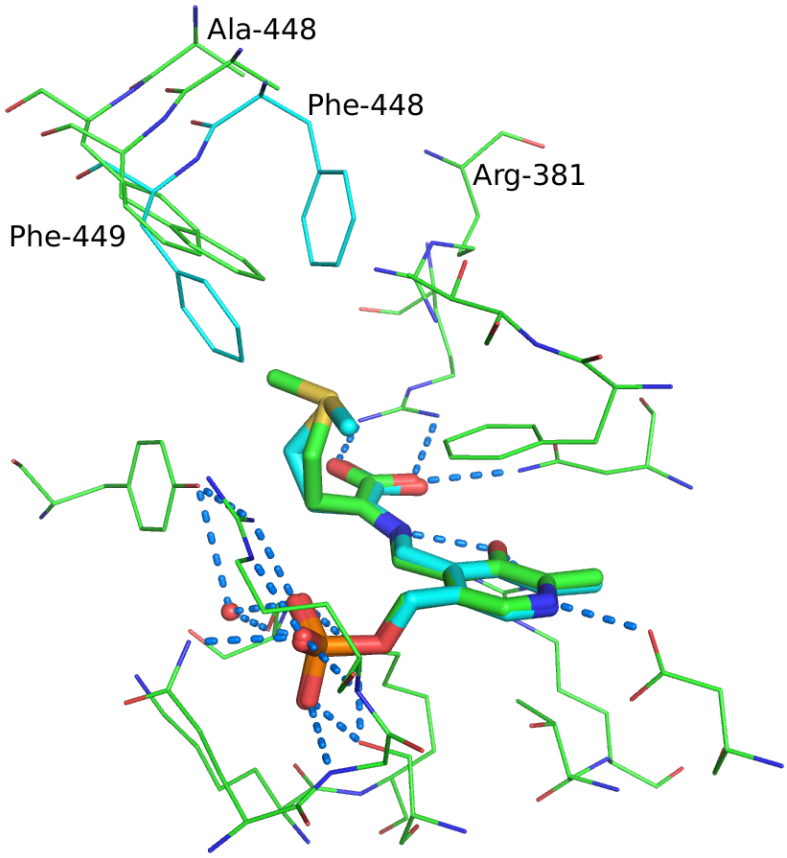

Figure 4. Structure of L-methionine bound to F448A TPL. F448A TPL is shown in green, and Phe-448, Phe-449 and the methionine complex of the wild-type TPL structure are shown in cyan. Potential hydrogen-bonds are indicated in blue dashes.

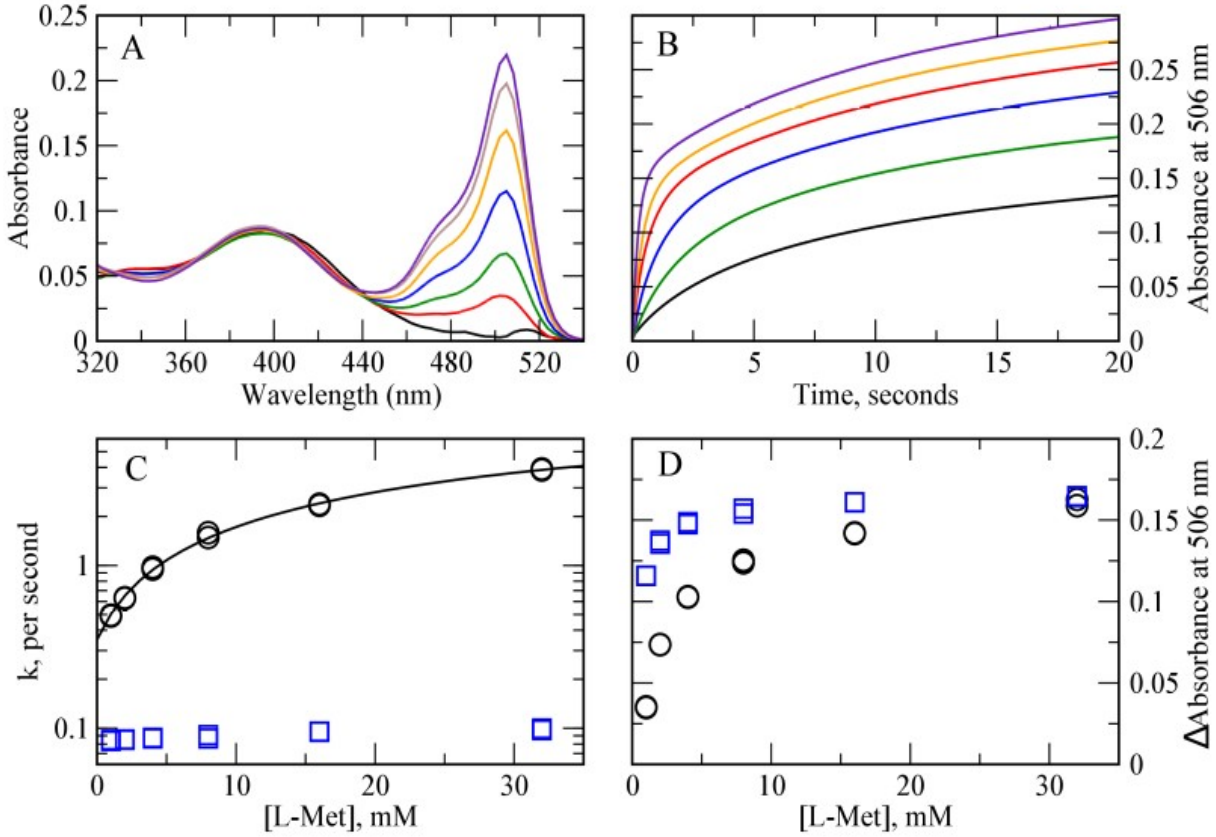

Figure 5. Stopped-flow kinetics of F448A TPL reaction with L-methionine. A. Rapid-scanning stopped-flow spectra of F448A TPL reaction with 0.05 M L-methionine. The scans are shown at 0.002 sec (black), 0.5 sec (red), 1 sec (green), 2 sec (blue), 4 sec (maroon), 8 sec (brown) and 12 sec (orange). B. Single-wavelength traces at 506 nm for the reaction at 1 (black), 2 (red), 4 (blue), 8 (green), 16 (orange), and 32 (brown) mM L-methionine. C. Rate constants for the reaction of L-methionine with F448A TPL fit to Eqn. 4 with two exponentials. Fast phase (○); slow phase (□). D. Amplitudes for the reaction of L-methionine with F448A TPL fit to Eqn. 4 with two exponentials. Fast phase (○); slow phase (□).

Structure of wild-type and F448A TPL complex with L-phenylalanine. The structure of wild-type TPL complexed with L-phenylalanine, a competitive inhibitor, has not been determined previously. We have now solved the structure of wild-type TPL complexed with L-phenylalanine to 1.8 Å. We find electron density for L-phenylalanine bound to PLP in both subunits. The density in chain A fits well to an expected quinonoid structure, with C_α nearly coplanar with the pyridine ring, and trigonal geometry of the C_α, C_β, and the carboxylate carbons (Figure S4A). The small domain of chain A is highly disordered in the complex (Figure S4C), showing density of both open and closed conformations. Refinement was attempted with both conformations separately, but significant unmodeled density remained in both cases. Hence, the structure of the L-phenylalanine complex was modeled with both open and closed conformations of chain A (Figure S4C) for residues 13-45, 348-377, 380-404, and 425-456, with significant reduction in R_{free} from 21 to 19.3%. The occupancies of the open and closed conformation of the refined structure are 56% and 44% for the open and closed conformations, respectively. Hence, we conclude that the open form is the major conformation of the L-phenylalanine quinonoid complex of chain A at equilibrium. In the open conformation, the side chain of Phe-449 is pointed out of the active site (Figure 6A, green). In the closed conformation, the side chain of Phe-449 moves about 8.5 Å, and is pointed in to the active site (Figure 6A, magenta), but the density is weak, indicating that it is disordered, probably because of steric clashes with the phenyl ring of the bound L-phenylalanine. Phe-448 does not change its conformation, but moves about 3.5 Å into the active site (Figure 6A, magenta). The side chain of Met-288 adopts two conformations depending on the position of Phe-449—it points in when Phe-449 points out, and vice versa. The side chain of Phe-36 changes conformation, and Arg-381 also moves closer to the bound ligand in the closed conformation. The NZ of Lys-257 is 3.6 Å from C_α of the bound amino acid, and forms hydrogen bonds with OG of Ser-51, OG of Ser-254, and an O of the phosphate of PLP (Figure 6A).

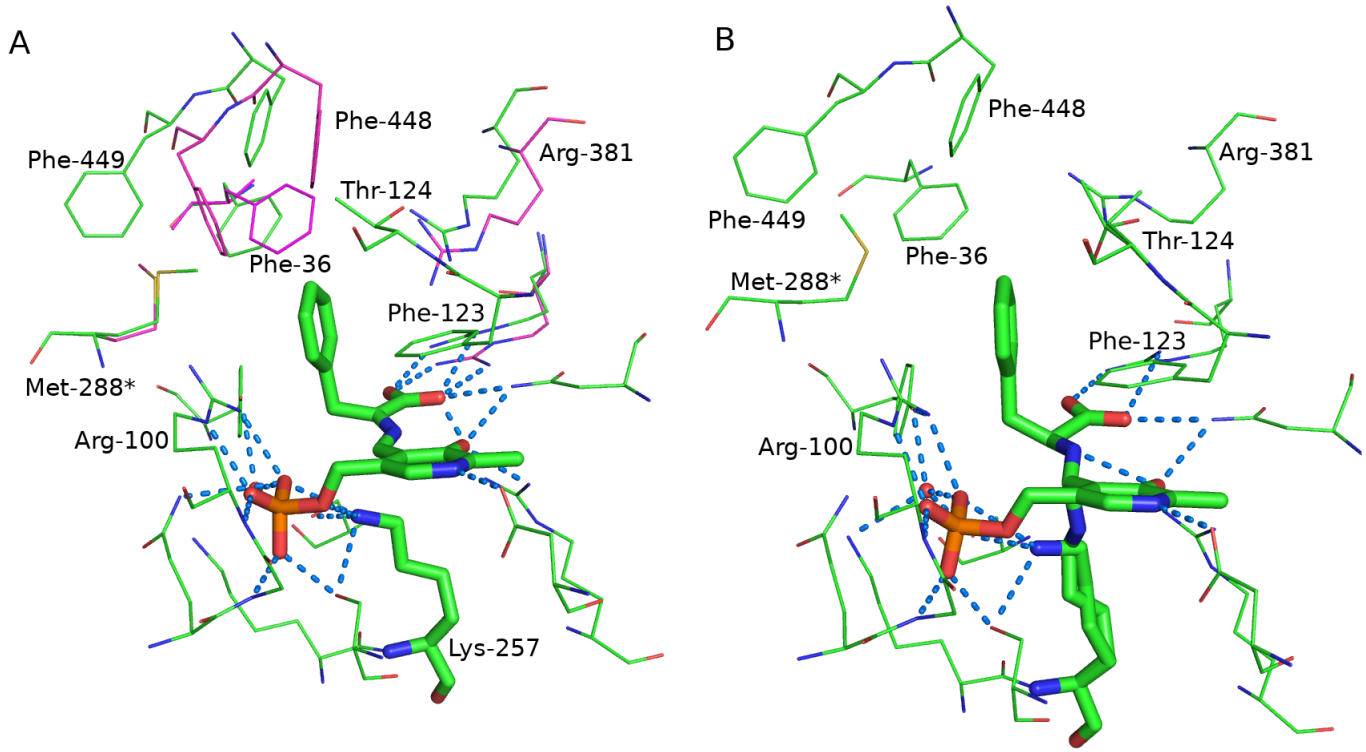

Figure 6. A. Structure of L-phenylalanine bound in chain A of wild-type TPL. The open conformation is shown in green and the closed conformation is shown in magenta. B. Structure of L-phenylalanine bound in the active site of chain B of wild-type TPL. Potential hydrogen-bonds are indicated in blue dashes.

In chain B, we find that the electron density fits best to an aldimine, with tetrahedral geometry at C_{α}, and the carboxylate out of plane with the PLP (Figure 6B), and there is also clear remaining electron density between the PLP C-4' and NZ of Lys-257 (Figure S4B), suggesting that there is an equilibrium mixture of external aldimine and either *gem*-diamine or internal aldimine complexes. The side chain of Lys-257 refines in two conformations, with 62% occupancy of the external aldimine, with 2.62 Å between the NZ and C4', and 38% occupancy, with an NZ to C4' distance of 1.64 Å. This suggests that the minor conformation of Lys-257 may be an internal aldimine, since the PLP would be rotated downward toward the Lys-257 NZ in that structure, reducing the NZ-C4' distance, or a *gem*-diamine. It should be noted that the internal aldimines of PLP-dependent enzymes are susceptible to

radiation damage due to strain (18, 19), so this may also contribute to the observed structure. As with other structures of TPL, the small domain of chain B is well ordered, and solely in an open conformation.

The structure of F448A TPL complexed with L-phenylalanine was solved to 2.27 Å. The L-phenylalanine in chain A is bound as a quinonoid complex (Figure 7A, Figure S5A), as was found for wild-type TPL. Although the active site is open, Phe-449 is pointed in, rather than out as it is for wild-type TPL (Figure 7A). Lys-257 forms hydrogen bonds with Ser-51, Ser-254, and the phosphate, similar to the structure of wild-type TPL complexed with L-phenylalanine. The disorder in the small domain of chain A of the L-phenylalanine complex of F448A TPL is similar to that of the wild-type TPL. However, we were not able to fit this structure to two conformations, since the two conformations converged on refinement to an open conformation. Thus, the open conformation must be the major conformation, showing again that the F448A mutation affects the conformational equilibrium of TPL. Similar to wild-type TPL, the L-phenylalanine in chain B is bound as an aldimine complex (Figure 7B, Figure S5B). However, for this complex there is only one conformation of Lys-257, with hydrogen bonds to OG of Ser-51, Ser-254, and the phosphate, and no residual electron density between Lys-257 and the PLP in chain B (Figure S5B).

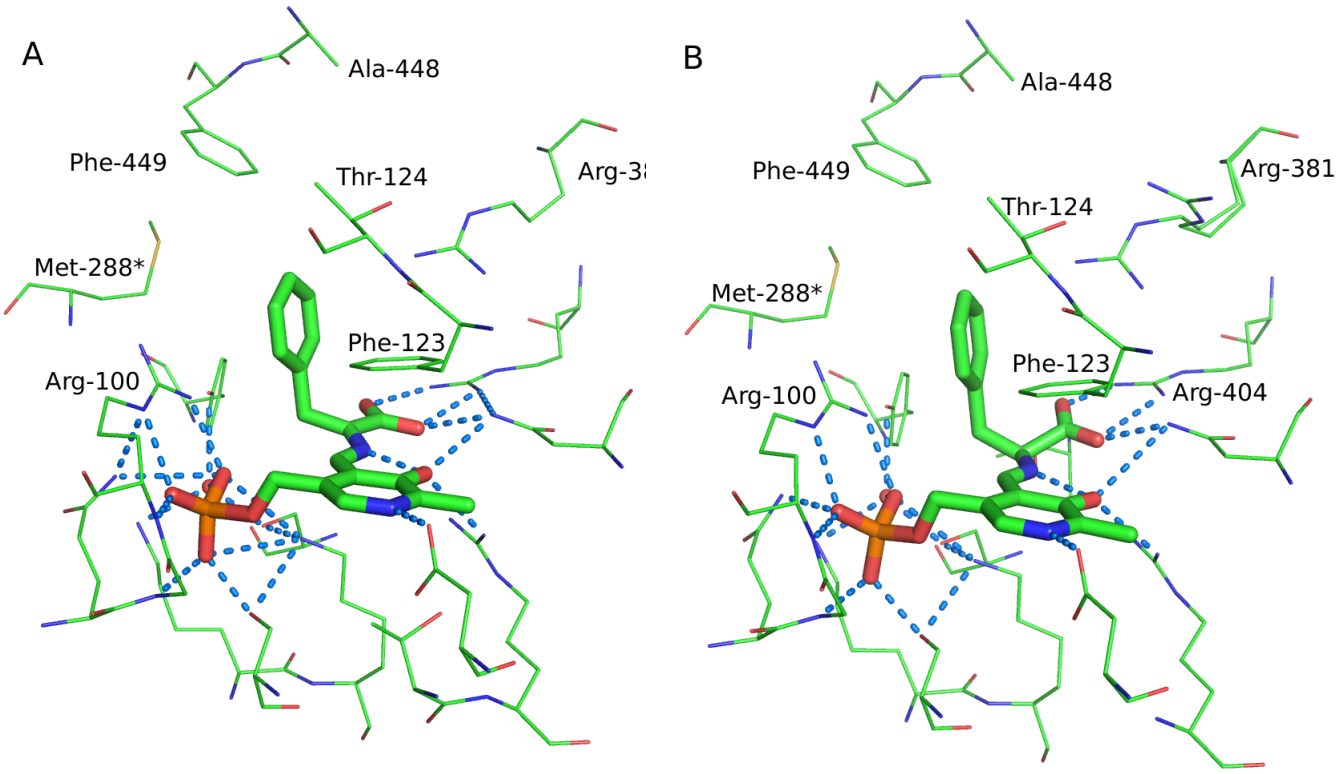

Figure 7. A. Structure of L-phenylalanine bound in chain A of F448A TPL. B. Structure of L-phenylalanine bound in the active site of chain B of F448A TPL. Potential hydrogen-bonds are indicated in blue dashes.

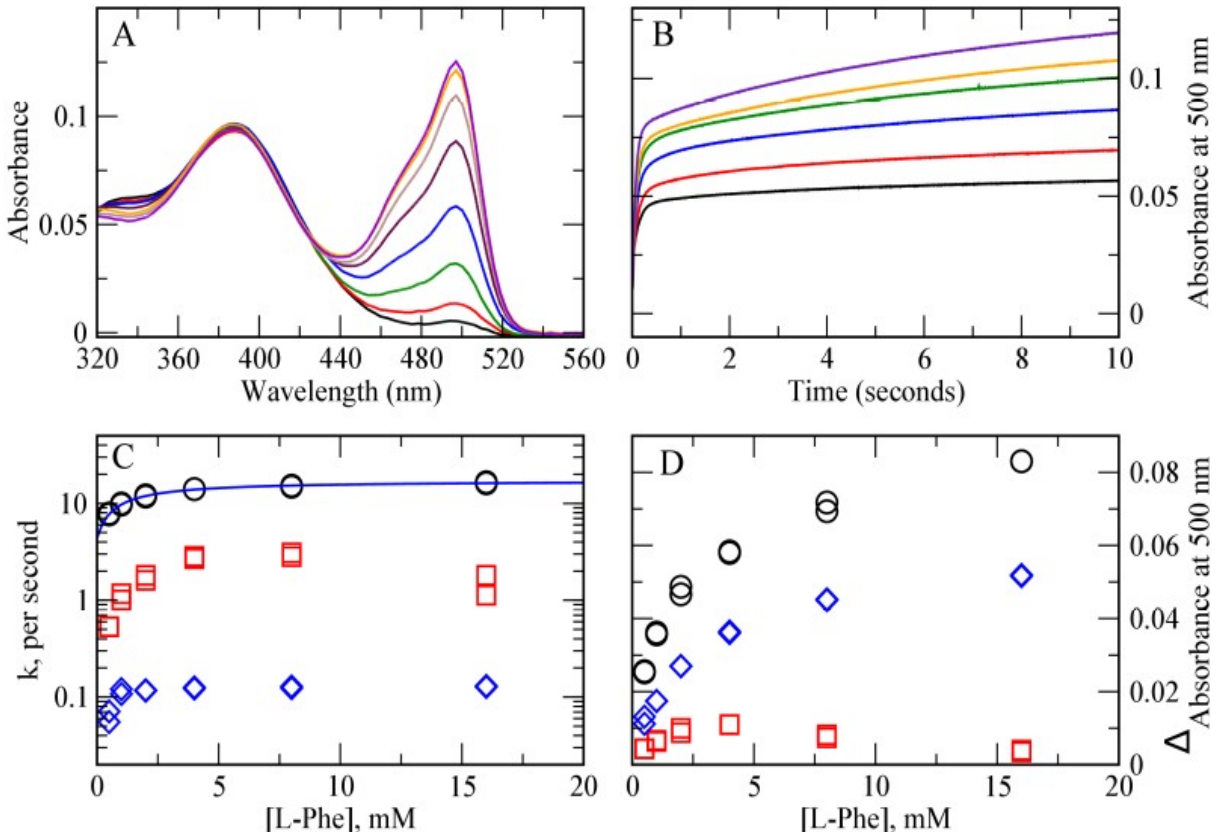

Figure 8. Stopped-flow kinetics of F448A TPL reaction with L-phenylalanine. A. Rapid-scanning stopped-flow spectra of F448A TPL reaction with 0.05 M L-phenylalanine. The scans are shown at 0.002 sec (black), 0.5 sec (red), 1 sec (green), 2 sec (blue), 4 sec (maroon), 8 sec (brown) and 12 sec (orange). B. Single-wavelength traces at 502 nm for the reaction at 0.5 (black), 1 (red), 2 (blue), 4 (green), 8 (orange), and 16 (brown) mM L-phenylalanine. C. Rate constants for the reaction of L-phenylalanine with F448A TPL fit to three exponentials. The line is the result of fitting to Eqn.4. Fast phase (○); intermediate phase (□); slow phase (◊). D. Amplitudes for the reaction of L-phenylalanine with F448A TPL fit to three exponentials. Fast phase (○); intermediate phase (□); slow phase (◊).

Kinetics of L-phenylalanine reaction with F448A TPL. The reaction kinetics of L-phenylalanine with wild-type TPL have been studied previously (19). The UV-visible spectra show that L-phenylalanine forms an equilibrating mixture of aldimine (~400 nm) and quinonoid (500 nm) complexes with wild-type TPL, as expected from the structure of the complex. The reaction of F448A TPL with L-phenylalanine is very similar (Figure 8A, 8B) to that of wild-type TPL. There is also a transient peak at about 340 nm that is likely due to a *gem*-diamine, since it is formed early in the reaction and decays as the quinonoid complex forms. The formation of the quinonoid intermediate, followed at 500 nm (Figure 8B) shows a dependence of both rate and amplitude on [L-phenylalanine] (Figure 8C, D). As we found with L-alanine, the reactions requires three exponentials to get a good fit to Eqn. 3. The two fastest phases show a hyperbolic dependence on [L-phenylalanine] (Figure 8C), and the phase with the intermediate rate constant has the lowest amplitude (Figure 8D). The fastest phase fits well to Eqn. 4, with k_f = 12.8 ± 0.5 s^{-1}, k_r = 4.4 ± 0.6 s^{-1}, and K_{eq} = 1.4 ± 0.2 mM. The values of k_f and k_r are comparable to those seen previously for L-phenylalanine with wild-type TPL, 16.2 s^{-1} and 6.4 s^{-1}, respectively (20). The intermediate phase does not fit well to Eqn. 4, probably because of the low amplitude. The slowest phase is nearly independent of [L-phenylalanine], with a rate constant of about 0.1 s^{-1}.

Structure of F448A TPL with 3-F-L-Tyrosine. The structures of other low activity mutant forms of TPL, F448H and Y71F, with bound 3-F-L-tyrosine, a good substrate for wild-type TPL, have been determined previously (7). The substrate is bound with the PLP in a quinonoid complex in these mutant enzymes. These structures show a significant distortion of the substrate aromatic ring about 20º out of plane with the C_β-C_γ bond. The strained complex is formed in the closed conformation by the juxtaposition of the phenyl side chains of Phe-448 and Phe-449 with the phenol ring of the substrate. Bending of the substrate ring to relieve these steric clashes results in formation of two new hydrogen bonds of the OH with Thr-124 and Arg-381, stabilizing the distorted geometry (7). In F448A TPL, we find that the 3-F-L-tyrosine in the A chain is in a quinonoid structure (Figure S6A), while the density in

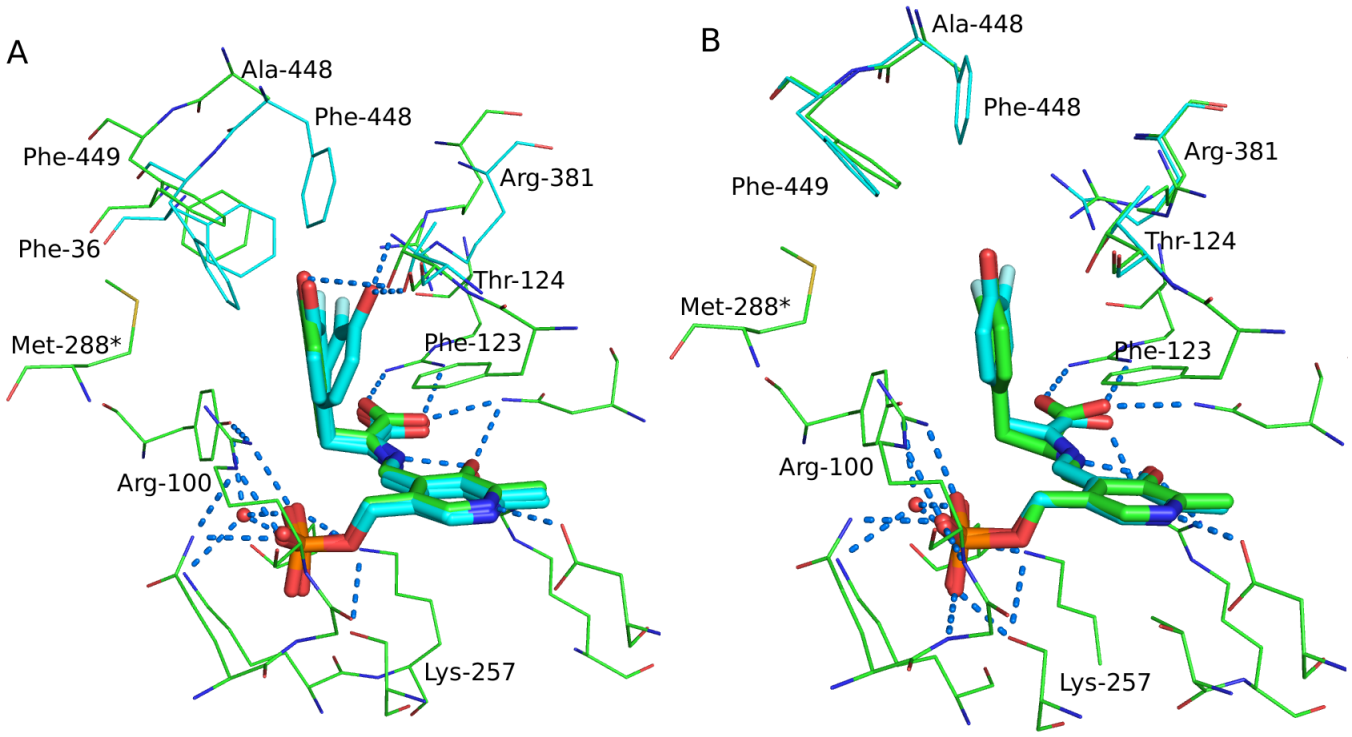

Figure 9. Structures of 3-F-L-tyrosine bound to F448A TPL. A. Structure of 3-F-L-tyrosine bound in the active site of Y71F (cyan) and F448A TPL (green). B. Structure of 3-F-L-tyrosine bound in the active site of chain B of Y71F (cyan) and F448A TPL (green). Potential hydrogen-bonds are indicated in blue dashes.

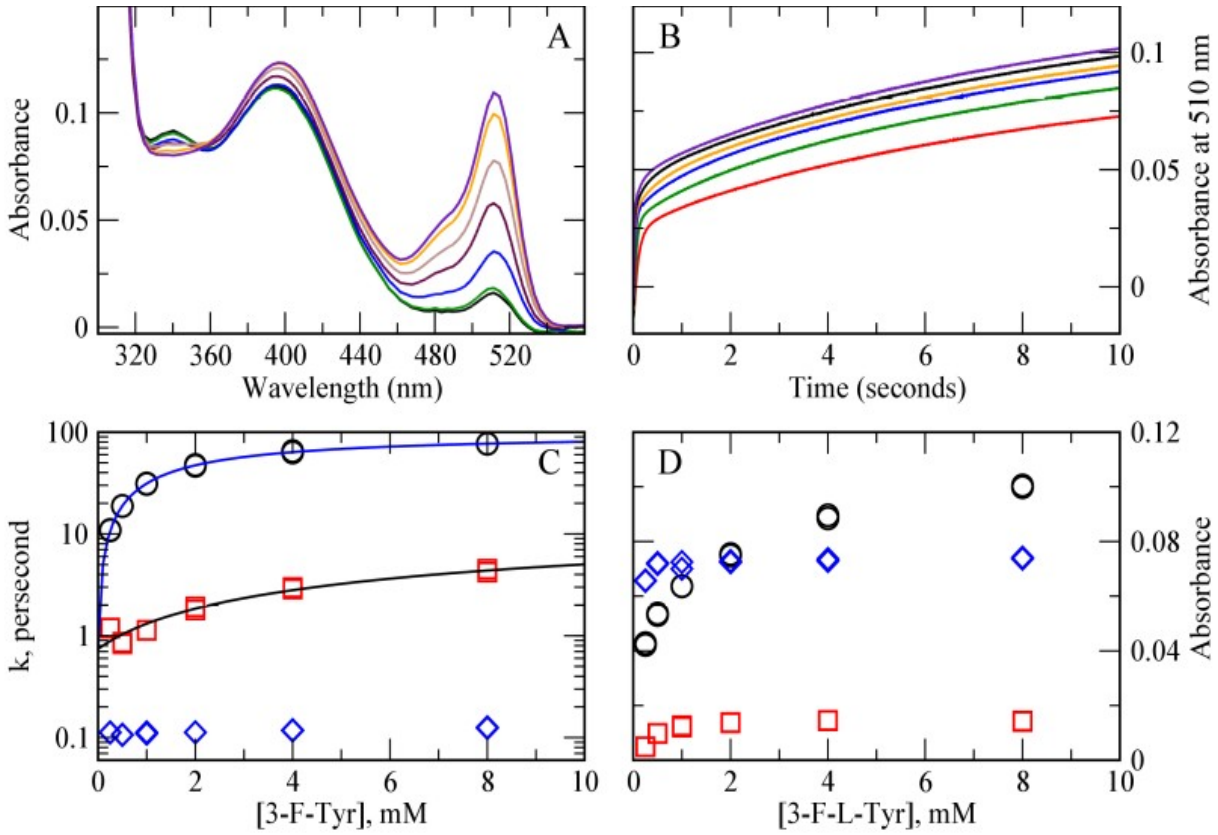

Figure 10. Stopped-flow kinetics of F448A TPL reaction with 3-F-L-tyrosine. A. Rapid-scanning stopped-flow spectra of F448A TPL reaction with 0.02 M 3-F-L-tyrosine. The scans are shown at 0.002 sec (black), 0.5 sec (red), 1 sec (green), 2 sec (blue), 4 sec (maroon), 8 sec (brown) and 12 sec (orange). B. Single-wavelength traces at 502 nm for the reaction at 0.25 (black), 0.5 (red), 1 (blue), 2 (green), 4 (orange), and 8 (brown) mM 3-F-L-tyrosine. C. Rate constants for the reaction of 3-F-L-tyrosine with F448A TPL. The lines are the fits to Eqn. 4. Fast phase (○); intermediate phase (□); slow phase (◊). D. Amplitudes for the reaction of 3-F-L-tyrosine with F448A TPL fit to three exponentials. Fast phase (○); intermediate phase (□); slow phase (◊).

the B chain fits best to an external aldimine (Figure S6B). We see no evidence for strain in the electron density for the bound 3-F-L-tyrosine. In fact, we initially modeled the bound substrate in the strained geometry found in Y71F and F448H TPL, but upon refinement it relaxed to the standard planar geometry of the aromatic ring. In chain A, the phenolic OH of the bound substrate is 3.6 Å from the OG of Thr-124, while it is 4.1 Å in chain B. In neither complex is there any significant remaining electron density at 1 σ between the NZ of Lys-257 and C4' of the PLP. Both chains of F448A TPL are in an open conformation, as can be seen from the positions of Phe-449 (Figure 9A, 9B, green), while the closed conformation of Y71F TPL has Phe-448 and Phe-449 moved toward the substrate about 3 Å (Figure 9A, cyan). Phe-36 has also moved toward the substrate about 1 Å in the Y71F structure (Figure 9A, cyan). Chain A has less disorder in the F448A TPL complex with 3-F-L-tyrosine than in the complex with L-phenylalanine (Compare Figure S5C and S6C). We were unable to fit these data to two conformations, so the structure was refined as the open conformation.

Kinetics of 3-F-L-tyrosine with F448A TPL. As expected from the crystal structure, the reaction of 3-F-L-tyrosine with F448A TPL results in the formation of a new absorption peak at 510 nm, attributable to a quinonoid structure (Figure 10A), as well as the external aldimine at 400 nm. There is a transient intermediate absorbing at 340 nm, which is likely a *gem*-diamine. The rate of the reaction is dependent on [3-F-L-tyrosine] (Figure 10B, 10C) and, as with L-phenylalanine, requires three exponentials to obtain a good fit to the data. The first two phases exhibit a hyperbolic dependence on [3-F-L-tyrosine]. As with the reaction of L-phenylalanine, the second phase has low amplitude. The kinetic parameters for the reaction of F448A TPL are similar to those found before with F448H TPL (20). The fast phase fits well to Eqn. 4, with $k_f = 97.1 \pm 0.9$ s^{-1}, $k_r = 0.7 \pm 0.7$ s^{-1}, and $K_{eq} = 2.2 \pm 0.1$ mM. The intermediate phase also fits to Eqn. 4, with $k_f = 15.3 \pm 9.3$ s^{-1}, $k_r = 0.7 \pm 0.1$ s^{-1}, and $K_{eq} = 25.7 \pm 20.5$ mM. The slow phase is relatively invariant with [3-F-L-tyrosine], with k about 0.1 s^{-1}. Since this slow phase is present in the reactions of all ligands and is concentration independent, it may be due to PLP dissociation upon dilution, and rebinding upon mixing with ligands.

Discussion

The reaction mechanism of TPL has been the subject of considerable interest, since it involves the β-elimination of a formally poor leaving group, with carbon-carbon bond cleavage. Earlier studies focused on the acid-base chemistry expected for the elimination reaction (4, 5, 20-24), and Tyr-71 was identified as the proximal proton donor to the phenol leaving group (3). Y71F TPL shows no detectable activity with L-tyrosine, but has measurable activity with SOPC (3). In addition, Arg-381 and Thr-124 were found to play a key role in the mechanism, since mutagenesis of these strictly conserved residues to alanine results in ~10^5 and ~10^3-fold losses in activity, respectively (19, 24). The structures of wild-type TPL and complexes with 3-(4-hydroxyphenyl)propionate, L-alanine and L-methionine have been determined previously (6, 7, 25-27). The structures showed that the strictly conserved residues, Phe-448 and Phe-449, are in the active site near the bound ligand. The structures of Y71F and F448H mutant TPL with 3-F-L-tyrosine showed that the substrate OH forms H-bonds to Arg-381 and Thr-124, as predicted from the mutagenesis results. Surprisingly, the substrate aromatic ring was found to be bent ~20º out of plane of the scissile C_β-C_γ bond in the complexes (7). The bending is in the direction of movement of the ring along the reaction coordinate in the β-elimination reaction, thus reducing activation energy. The strain is introduced by the movement of Phe-448 and Phe-449 into van der Waals contact with the substrate in the active site in the closed conformation. In F448H, the imidazole ring can form an additional H-bond with the substrate OH in the strained geometry, stabilizing the complex (7). Thus, we subsequently studied mutations with smaller neutral side chains, F448A, F448L, and F449A, to probe the role of steric effects in the reaction. These mutations were found to have significant (>10^3) effects on the elimination of L-tyrosine, but much smaller effects (~10%) on the elimination of S-ethyl-L-cysteine and S-(*o*-nitrophenyl)-L-cysteine (8). We concluded that these results are consistent with a mechanism wherein ground-state strain induced by these phenylalanine residues contributes up to 50% of the activation energy reduction required for the rate acceleration of phenol elimination from L-tyrosine (8).

TPL is a member of the aminotransferase superfamily of PLP-dependent enzymes (28). The enzymes in this family have been shown to form closed active sites during the catalytic cycle (29, 30). The quinonoid structures previously determined of wild-type TPL bound to L-alanine and L-methionine are in closed active site conformations. We have now obtained crystal structures of F448A TPL and its complexes with inhibitors, L-alanine, L-methionine, and L-phenylalanine, and a substrate, 3-F-L-tyrosine. The F448A mutation has only minor effects on the protein backbone (Figure 1), but does significantly increase the disorder in the small domain, as reflected in the higher B-factors for F448A TPL and its complexes (Table 1 and Figure S1). This disorder is centered in the small domain of chain A in residues 13-45, the loop containing residues 388-394, and the C-terminus from residue 435-456. The complex of wild-type TPL with L-phenylalanine and the complex of L-methionine with F448A TPL were refined as a nearly equal mixture of open and closed conformations, and have lower B-factors as a result. The F448A TPL complexes of L-alanine, L-phenylalanine, and 3-F-L-tyrosine do not refine as multiple conformations, so the closed conformations must have lower occupancy than the open conformations. This conformational mobility of TPL has been seen previously, and other structures have been refined as multiple conformations in chain A (18).

In the closed conformation, there would be steric clashes of the side chains of Phe-448 and Phe-449 with the phenyl ring of the bound L-phenylalanine that do not exist in the complexes of L-alanine and L-methionine. The closed conformation is disfavored for L-phenylalanine because the steric strain associated with active site closure cannot be compensated by hydrogen bonding with Thr-124 and Arg-381, as does L-tyrosine or 3-F-L-tyrosine. Since the steric clashes are not relieved, the closed conformation is destabilized. However, the complex of F448A TPL with L-phenylalanine also does not form a closed conformation, even though the steric clash of Ala-448 with the bound ligand would be minimized. This observation, together with the structures of the F448A TPL with L-alanine and L-methionine, shows that the Phe-448 to alanine mutation affects the equilibrium between open and closed conformations of TPL.

F448A TPL has a k_{cat} with L-tyrosine reduced by ~10^4, while S-ethyl-L-cysteine and SOPC have k_{cat} values reduced 8-fold and 3-fold, respectively (8). Both of these alternative substrates have good leaving groups, ethanethiol and 2-nitrothiophenol, respectively, that do not require activation. The elimination of these thiols should only require formation of the quinonoid complex, and our data show that F448A is capable of forming quinonoid complexes with rate constants similar to those of wild-type TPL (Reference 8 and Figures 3, 5, 8, 10). The rate constants for C_α deprotonation of the amino acid ligands of TPL depend on the structure of the side chain. Using the values of k_f from the exponential fits of the fast phase of quinonoid intermediate formation to Eqn. 4, these values are ~1, 12.1, 12.8, and 97 s^{-1} for L-alanine, L-methionine, L-phenylalanine and 3-F-L-tyrosine, respectively. The rate constants for L-phenylalanine and 3-F-L-tyrosine deprotonation by F448A TPL are in good agreement with the values for wild-type TPL, 16 and 120 s^{-1}, respectively (8, 20). Formation of quinonoid intermediates is not dependent on the closed conformation, since the structures of complexes of F448A TPL are all in open conformations. The dependence of k_f on side chain structure suggests that there are favorable interactions between the substrate side chain and the active site in the open as well as closed conformation. An increase in the rate of quinonoid complex formation of ~100-fold between L-alanine and 3-F-L-tyrosine is consistent with ~3 kcal/mol lower activation energy, which could arise from favorable dipolar or van der Waals interactions of the side chain with the active site in the quinonoid complex. The phenyl ring of bound L-phenylalanine can have potential T-shaped π-π interactions (31) with the perpendicular phenyl ring of Phe-123 (3.5 Å), and π-cation interactions (32) with the guanidine of Arg-100 (3.1 Å), which may contribute to the observed higher rate of quinonoid formation for L-phenylalanine than L-alanine. Electronic effects of the aromatic ring may also contribute to the faster reaction of L-phenylalanine. It is less clear why L-methionine reacts faster than L-alanine, since there are no obvious contacts of the side chain with the active site. This may be due to electron withdrawing effects of the thioether.

In the structure of 3-F-L-tyrosine bound to F448A TPL, the distance between the substrate OH and the OG of Thr-124 decreases from 4.1 Å in the external aldimine complex to 3.6 Å in the quinonoid complex, consistent with a hydrogen bond. The formation of this hydrogen bond in the quinonoid intermediate probably explains the much faster rate of C_α deprotonation of phenolic substrates, L-tyrosine and 3-F-L-tyrosine, than inhibitory amino acids by TPL. It is interesting that the other 3-halotyrosines show much slower rate constants, ~6 s^{-1}, for quinonoid intermediate formation (33), suggesting that the steric bulk of the larger halogens affects hydrogen bond formation with Thr-124. The alanine mutant of Thr-124 shows a k_f value for tyrosine deprotonation comparable to that of

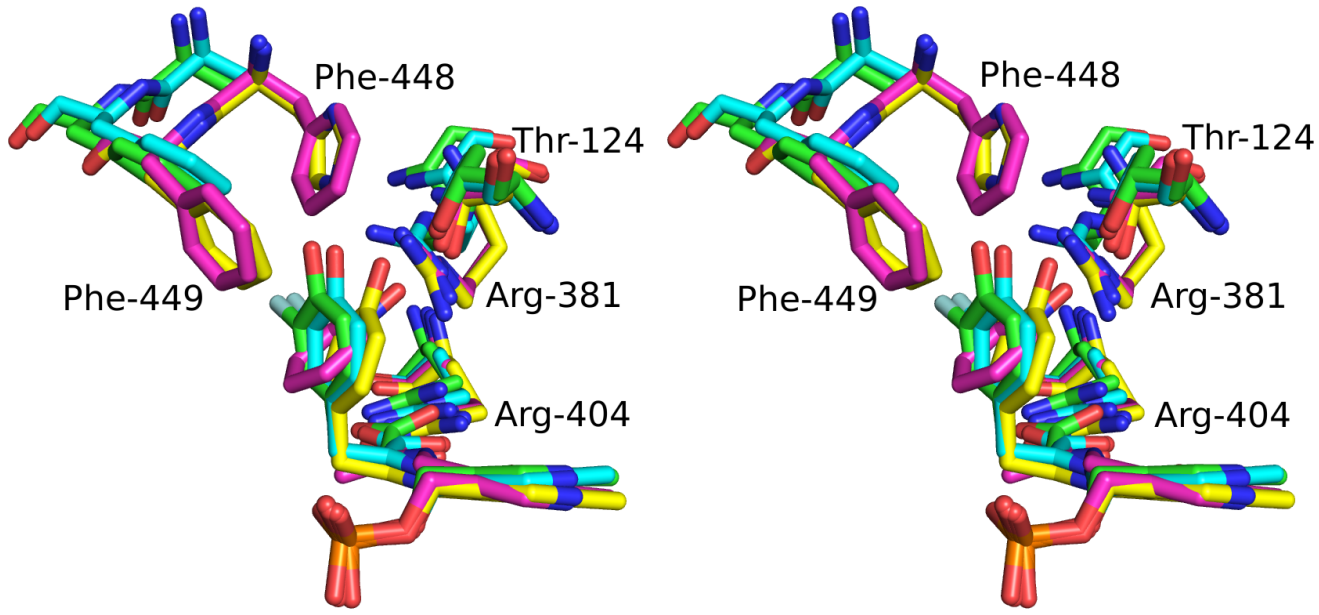

Figure 11. Crossed-eye stereo view of the overlay of the 3-F-L-tyrosine complexes of F448A TPL and F448H TPL with the wild-type TPL complex with L-alanine and pyridine N-oxide. Green: External aldimine of 3-F-L-tyrosine with F448A TPL. Cyan: Quinonoid complex of 3-F-L-tyrosine with F448A TPL. Yellow, F448H TPL complex with 3-F-L-tyrosine. Magenta: wild-type TPL complex with L-alanine and pyridine N-oxide.

phenylalanine, consistent with a role of hydrogen bonding (20). In the strained quinonoid complex of 3-F-L-tyrosine with Y71F and F448H TPL, the distance between the substrate OH and OG of Thr-124 is further reduced to 2.6 Å (Figure 11) (7), indicating that this hydrogen bond becomes even stronger in the closed conformation of the quinonoid intermediate, and an additional hydrogen bond is formed with Arg-381. The conformation of Arg-381 changes to form this hydrogen bond (Figure 11, yellow structure).

Elimination of phenol from L-tyrosine must take place within the closed active site conformation. The active site closing introduces strain in the substrate which is relieved in the transition state leading to the products, phenol and the aminoacrylate. A product analogue, pyridine-N-oxide, bound to the L-alanine quinonoid complex, is in a closed conformation with the N-O hydrogen bonded to Thr-124 and Arg-381 (Figure 11, magenta structure) (7). This structure mimics the phenol-aminoacrylate product complex immediately after C_β-C_γ bond cleavage. In proceeding on the reaction coordinate from external aldimine to open quinonoid intermediate to closed quinonoid intermediate, there is coordinated movement of the substrate phenyl ring toward the final position of the phenol product, as can be seen by overlay of the structures of these intermediates (Figure 11). The order of product release is phenol first, followed by pyruvate, as shown by the stabilization of aminoacrylate intermediates by 4-hydroxypyridine, an isoelectronic analogue of phenol (33). This suggests that the release of phenol triggers opening of the active site, allowing the iminopyruvate product to be released. The mutation of Phe-448 to alanine apparently affects the equilibrium of open and closed conformations as well as reduces the ground-state strain in the bound L-tyrosine substrate. It is likely that the elimination mechanism of the non-physiological substrates like SOPC also requires a closed active site. Since there is less than a 10-fold effect of the F448A mutation on the k_{cat} values of S-ethyl-L-cysteine and SOPC, it is likely that the conformational equilibrium is affected by the mutation by less than a factor of ten. The remainder of the effect of the F448A mutation on the reaction of L-tyrosine, $\geq 10^3$, must be due to the reduction in ground-state strain.

Scheme 1

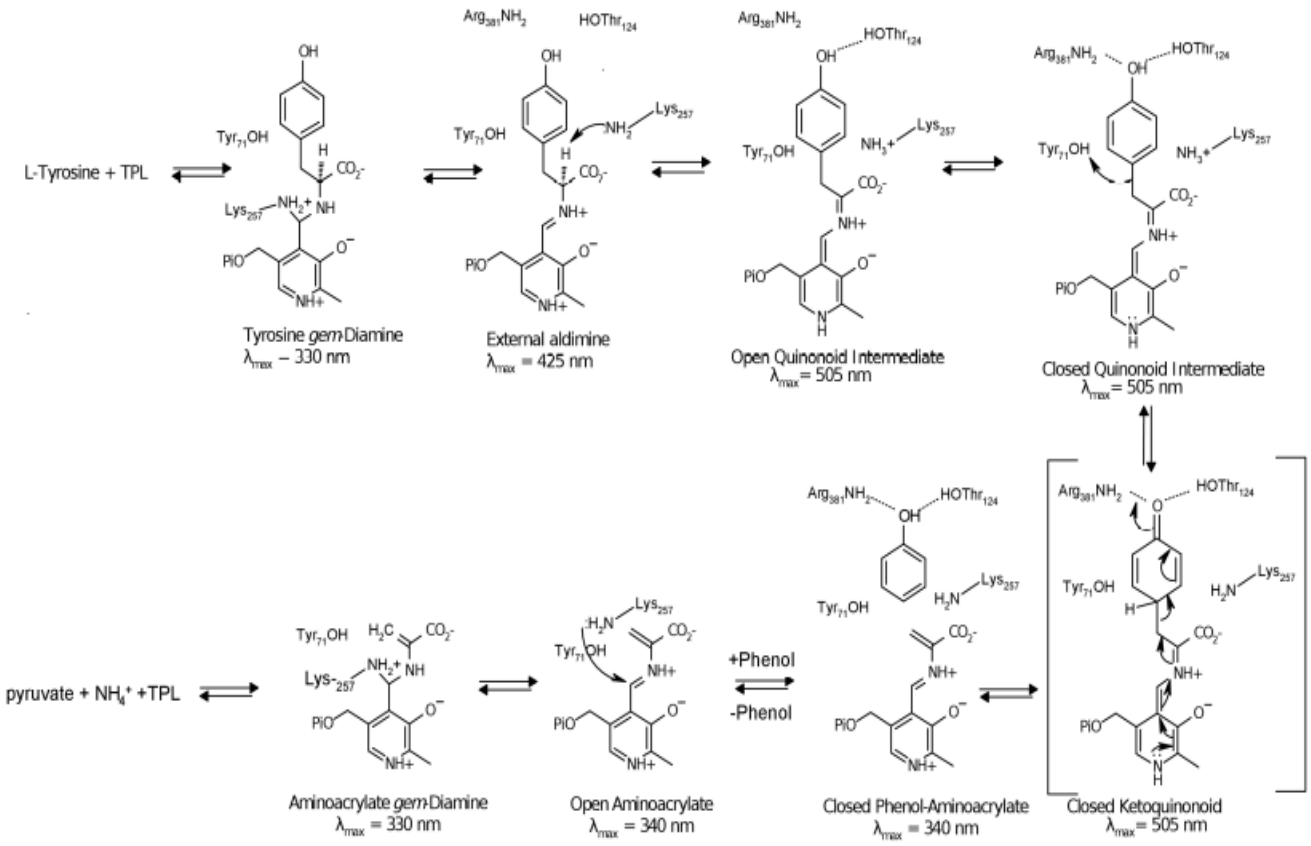

The proposed reaction mechanism based on the structural results obtained in this work and previous studies is shown in Scheme 1. The initial binding of L-tyrosine with PLP forms a *gem*-diamine complex, which then releases Lys-257 in the neutral form to give the external aldimine. Deprotonation of the C_α-H by Lys-257 then forms a quinonoid complex, initially in an open conformation, with formation of the hydrogen bond to Thr-124. The closed active site then forms by movement of the small domain towards the large domain, introducing the strain, shortening the hydrogen-bond to Thr-124, and forming a new hydrogen bond with Arg-381. In the quinonoid complex, the protonated Lys-257 forms hydrogen bonds with Ser-51, Ser-254, and the phosphate (Figure 12). The proton transferred to the phenol leaving group ultimately arises from Lys-257 through the network of H-bonds with Ser-51 and a water connecting it to Tyr-71, which is located 3.2 Å from C_γ of the scissile bond (Figure 12). This hydrogen bonding network is likely responsible for the observed small (5-20%) internal return of the C_α deuteron to the phenol product (5, 22).

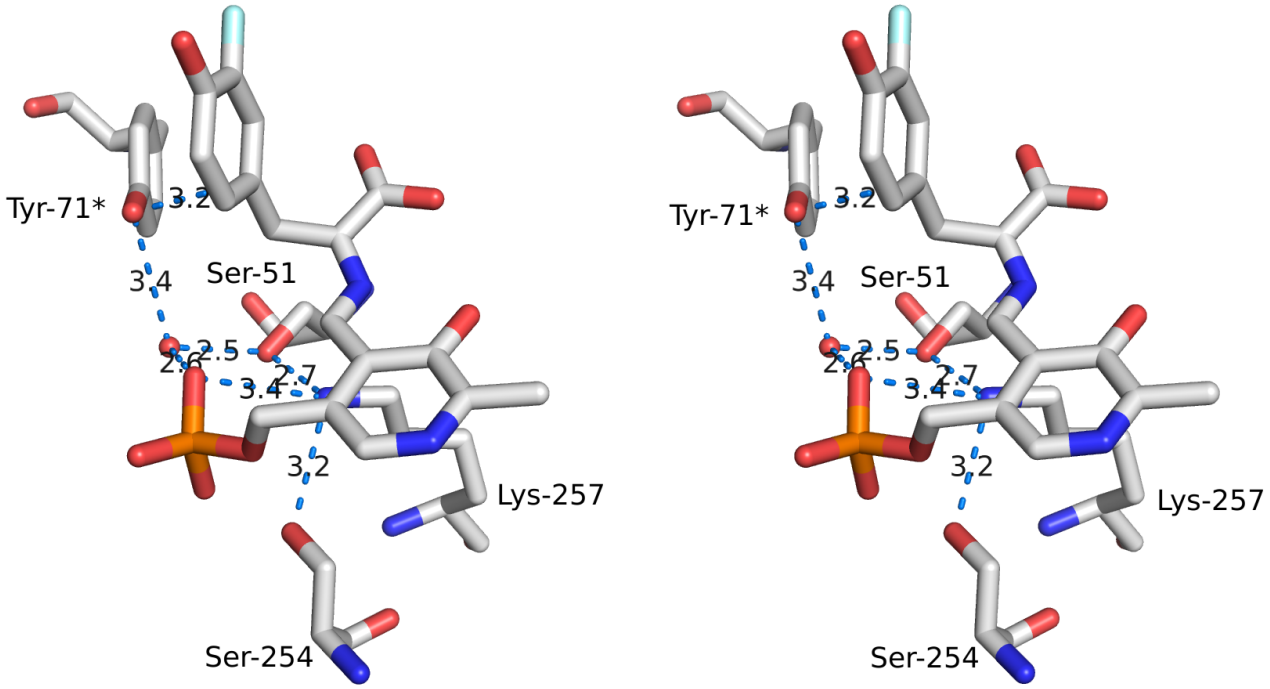

Figure 12. Crossed-eye stereo view of the hydrogen bonding network connecting Lys-257 to Tyr-71 of the quinonoid complex of F448A TPL with 3-F-L-tyrosine in chain A. The numbers are the distances in Å between the atoms.

Although stereochemical and labeling studies of TPL suggested that the elimination occurs with a *syn* relationship between the abstracted C_α-H bond and the leaving group due to observed internal return of the C_α-H to the phenol leaving group (5), our structures here, and previously (7), show that the C_α-H bond and the leaving phenyl ring of the substrate have an *anti* orientation (Figure 9). Ser-51 was found previously to be essential for formation of quinonoid species and in elimination (34). Figure 12 shows that Ser-51 plays a crucial role in stabilizing the quinonoid complex by hydrogen bonding to the protonated Lys-257, as well as acting as a conduit for transfer of a proton by a Grotthus mechanism to the leaving group to C_γ via a water and Tyr-71. The pyramidalization of C_γ induced by the strain increases basicity and facilitates formation of a ketoquinonoid species (Scheme 1). This may be a short-lived intermediate or a transition state. Kinetic studies of the mechanistically very similar

enzyme, tryptophan indole-lyase, suggested that the ring protonation and carbon-carbon bond cleavage are concerted (35). Elimination then occurs, producing an aminoacrylate intermediate with phenol bound by hydrogen bonding to Thr-124 and Arg-381. Release of the phenol product results in opening of the active site, formation of a *gem*-diamine by attack of Lys-257 on the aminoacrylate, and release of the product, most likely as iminopyruvate, since the methyl group of the pyruvate product is formed stereospecifically, with retention of configuration (5).

Conclusions. F448A TPL forms quinonoid complexes with L-alanine, L-methionine, L-phenylalanine, and 3-F-L-tyrosine, as does wild-type TPL. The structures of these complexes are all very similar with those of wild-type TPL. However, these complexes are all in open conformations, whereas wild-type TPL forms closed conformations with L-alanine and L-methionine, but not L-phenylalanine. Thus, the Phe-448 to alanine mutation affects the conformational equilibrium. The kinetics of intermediate formation are similar for both wild-type and F448A TPL, showing that the mutation does not significantly affect formation of quinonoid complexes. The faster kinetics for quinonoid intermediate formation of L-tyrosines by wild-type and F448A TPL is likely due to formation of a hydrogen bond with Thr-124. The structure of 3-F-L-tyrosine bound to F448A TPL does not show the substrate strain seen previously with F448H and Y71F TPL. These structural data are consistent with the previously suggested role of Phe-448 to introduce ground-state strain in the substrate (7, 8).

Acknowledgments. Data were collected at Southeast Regional Collaborative Access Team (SER-CAT) 22-ID and 22-BM beamlines at the Advanced Photon Source, Argonne National Laboratory, and the University of Georgia X-ray diffraction Core Facility (XRDC). SER-CAT is supported by its member institutions (see www.ser-cat.org/members.html) and equipment grants (S10 RR25528) and S10 RR028976) from the National Institutes of Health. Use of the Advanced Photon Source was supported by the U. S. Department of Energy, Office of Science, Office of Basic Energy Sciences, under Contract No. W-31-109-Eng-3. The XRDC is supported by its UGA member groups (x-ray.uga.edu) and an equipment grant (S10 OD021762) from the National Institutes of Health.

Supporting information. Ribbon structures colored by B-factor; electron density maps of the bound ligands; comparison of electron density maps refined with one or two alternate conformations.

References

1. Kumagai, H., Yamada, H., Matsui, H., Ohkishi, H., & Ogata, K. (1970). Tyrosine phenol lyase I. Purification, crystallization, and properties. *J. Biol. Chem., 245*, 1767-1772.
2. Nagasawa, T., Utagawa, T., Goto, J., Kim, C. J., Tani, Y., Kumagai, H., & Yamada, H. (1981). Syntheses of L-Tyrosine Related Amino Acids by Tyrosine Phenol-lyase of *Citrobacter intermedius*. *FEBS J., 117*, 33-40.
3. Chen, H. Y., Demidkina, T. V., & Phillips, R. S. (1995). Site-directed mutagenesis of tyrosine-71 to phenylalanine in *Citrobacter freundii* tyrosine phenol-lyase: evidence for dual roles of tyrosine-71 as a general acid catalyst in the reaction mechanism and in cofactor binding. *Biochemistry, 34*, 12276-12283.
4. Kiick, D. M., & Phillips, R. S. (1988). Mechanistic deductions from kinetic isotope effects and pH studies of pyridoxal phosphate dependent carbon-carbon lyases: *Erwinia herbicola* and *Citrobacter freundii* tyrosine phenol-lyase. *Biochemistry, 27*, 7333-7338.
5. Palcic, M. M., Shen, S. J., Schleicher, E., Kumagai, H., Sawada, S., Yamada, H., & Floss, H. G. (1987). Stereochemistry and mechanism of reactions catalyzed by tyrosine phenol-lyase from *Escherichia intermedia*. *Zeit. Natur. C, 42*, 307-318.
6. Milić, D., Demidkina, T. V., Faleev, N. G., Matković-Čalogović, D., & Antson, A. A. (2008). Insights into the catalytic mechanism of tyrosine phenol-lyase from X-ray structures of quinonoid intermediates. *J. Biol. Chem., 283*, 29206-29214.
7. Milic, D., Demidkina, T. V., Faleev, N. G., Phillips, R. S., Matkovic-Calogovic, D., & Antson, A. A. (2011). Crystallographic snapshots of tyrosine phenol-lyase show that substrate strain plays a role in C–C bond cleavage. *J. Am. Chem. Soc., 133*, 16468-16476.
8. Phillips, R. S., Vita, A., Spivey, J. B., Rudloff, A. P., Driscoll, M. D., & Hay, S. (2016). Ground-State Destabilization by Phe-448 and Phe-449 Contributes to Tyrosine Phenol-Lyase Catalysis. *ACS Catalysis, 6*, 6770-6779.

9. Chen, H., Gollnick, P., & Phillips, R. S. (1995). Site-Directed Mutagenesis of His343→ Ala in *Citrobacter freundii* Tyrosine Phenol-Lyase. *FEBS J, 229*, 540-549.

10. Phillips, R. S., Demidkina, T. V., Zakomirdina, L. N., Bruno, S., Ronda, L., & Mozzarelli, A. (2002). Crystals of tryptophan indole-lyase and tyrosine phenol-lyase form stable quinonoid complexes. *J. Biol. Chem., 277*, 21592-21597.

11. Kabsch, W. XDS. *Acta Cryst. D66*, 125-132 (2010).

12. Karplus, P. A., & Diederichs, K. (2012). Linking crystallographic model and data quality. *Science, 336*, 1030-1033.

13. McCoy, A. J., Grosse-Kunstleve, R. W., Adams, P. D., Winn, M. D., Storoni, L. C., & Read, R. J. (2007). Phaser crystallographic software. *J. Appl. Cryst., 40*, 658-674.

14. Emsley, P., & Cowtan, K. (2004). Coot: model-building tools for molecular graphics. *Acta Cryst. D: Biol. Cryst., 60*, 2126-2132.

15. Afonine, P. V., Grosse-Kunstleve, R. W., Echols, N., Headd, J. J., Moriarty, N. W., Mustyakimov, M., ... & Adams, P. D. (2012). Towards automated crystallographic structure refinement with phenix. refine. *Acta Cryst. D: Biol. Cryst., 68*, 352-367.

16. Kumagai, H., Kashima, N., & Yamada, H. (1970). Racemization of D-or L-alanine by crystalline tyrosine phenol-lyase from *Escherichia intermedia*. *Biochem. Biophys. Res. Comm., 39*, 796-801.

17. Chen, H., & Phillips, R. S. (1993). Binding of phenol and analogs to alanine complexes of tyrosine phenol-lyase from *Citrobacter freundii*: Implications for the mechanisms of. alpha.,. beta.-elimination and alanine racemization. *Biochemistry, 32*, 11591-11599.

18. https://bib.irb.hr/datoteka/472684.Dalibor_Milic_Doctoral_Thesis.pdf.

19. Dubnovitsky, A. P., Ravelli, R. B. G., Popov, A. N. & Papageorgiou, A. C. (2005) Strain relief at the active site of phosphoserine aminotransferase induced by radiation damage. *Protein Sci*. *14*, 1498-1507.

20. Demidkina, T. V., Barbolina, M. V., Faleev, N. G., Sundararaju, B., Gollnick, P. D., & Phillips, R. S. (2002). Threonine-124 and phenylalanine-448 in *Citrobacter freundii* tyrosine phenol-lyase are necessary for activity with L-tyrosine. *Biochem. J., 363*, 745-752.

21. Muro, T., Nakatani, H., Hiromi, K., Kumagai, H., & Yamada, H. (1978). Elementary processes in the interaction of tyrosine phenol lyase with inhibitors and substrate. *J. Biochem., 84*, 633-640.

22. Faleev, N. G., Lyubarev, A. E., Martinkova, N. S., & Belikov, V. M. (1983). Mechanism and stereochemistry of α,β-elimination of l-tyrosine catalysed by tyrosine phenol-lyase. *Enz. Microb. Technol*., 5, 219-224.

23. Faleev, N. G., Axenova, O. V., Demidkina, T. V., & Phillips, R. S. (2003). The role of acidic dissociation of substrate's phenol group in the mechanism of tyrosine phenol-lyase. *Biochim. Biophys. Acta (BBA)-Prot. Proteom., 1647*, 260-265.

24. Faleev, N. G., Spirina, S. N., Demidkina, T. V., & Phillips, R. S. (1996). Mechanism of catalysis by tyrosine phenol lyase from *Erwinia herbicola*. Multiple kinetic isotope effects for the reactions with adequate substrates. *J. Chem. Soc., Perkin 2*, 2001-2004.

25. Sundararaju, B., Antson, A. A., Phillips, R. S., Demidkina, T. V., Barbolina, M. V., Gollnick, P., Dodson, G. G. & Wilson, K. S. (1997). The crystal structure of *Citrobacter freundii* tyrosine phenol-lyase complexed with 3-(4'-hydroxyphenyl) propionic acid, together with site-directed mutagenesis and kinetic analysis, demonstrates that arginine 381 is required for substrate specificity. *Biochemistry, 36*, 6502-6510.

26. Antson, A. A., Demidkina, T. V., Gollnick, P., Dauter, Z., Von Tersch, R. L., Long, J., Berezhnoy, S. N., Phillips, R. S., Harutyunyan, E. H. & Wilson, K. S. (1993). Three-dimensional structure of tyrosine phenol-lyase. *Biochemistry, 32*, 4195-4206.

27. Milić, D., Matković-Čalogović, D., Demidkina, T. V., Kulikova, V. V., Sinitzina, N. I., & Antson, A. A. (2006). Structures of apo-and holo-tyrosine phenol-lyase reveal a catalytically

critical closed conformation and suggest a mechanism for activation by K+ ions. *Biochemistry, 45*, 7544-7552.

28. Alexander, F. W., Sandmeier, E., Mehta, P. K., & Christen, P. (1994). Evolutionary relationships among pyridoxal□5′□phosphate□dependent enzymes. *FEBS J., 219*, 953-960.
29. McPhalen, C. A., Vincent, M. G., Picot, D., Jansonius, J. N., Lesk, A. M., & Chothia, C. (1992). Domain closure in mitochondrial aspartate aminotransferase. *J. Mol. Biol., 227*, 197-213.
30. Jäger, J., Moser, M., Sauder, U., & Jansonius, J. N. (1994). Crystal structures of *Escherichia coli* aspartate aminotransferase in two conformations: comparison of an unliganded open and two liganded closed forms. *J. Mol. Biol., 239*, 285-305.
31. Hunter, C. A., & Sanders, J. K. (1990). The nature of. pi.-. pi. interactions. *J. Am. Chem. Soc.*, *112*, 5525-5534.
32. Gallivan, J. P., & Dougherty, D. A. (1999). Cation-π interactions in structural biology. *Proc. Natl. Acad. Sci.*, *96*, 9459-9464.
33. Phillips, R. S., Chen, H. Y., & Faleev, N. G. (2006). Aminoacrylate intermediates in the reaction of *Citrobacter freundii* tyrosine phenol-lyase. *Biochemistry, 45*, 9575-9583.
34. Barbolina, M. V., Kulikova, V. V., Tsvetikova, M. A., Anufrieva, N. V., Revtovich, S. V., Phillips, R. S., Gollnick, P. D., Demidkina, T. V. & Faleev, N. G. (2018). Serine 51 residue of *Citrobacter freundii* tyrosine phenol-lyase assists in C-α-proton abstraction and transfer in the reaction with substrate. *Biochimie*, *147*, 63-69.
35. Phillips, R. S., Sundararaju, B., & Faleev, N. G. (2000). Proton transfer and carbon−carbon bond cleavage in the elimination of indole catalyzed by *Escherichia coli* tryptophan indole-lyase. *J. Am. Chem. Soc.*, *122*, 1008-1014.

Table of Contents Graphic